

Spatiotemporal features of human mobility

James P. Bagrow^{1,2} and Yu-Ru Lin^{3,4}

¹Engineering Sciences and Applied Mathematics, Northwestern University, Evanston, IL 60208, USA

²Center for Complex Network Research, Northeastern University, Boston, MA 02115, USA

³College of Computer and Information Science, Northeastern University, Boston, MA, 02115, USA

⁴Institute for Quantitative Social Science, Harvard University, Cambridge, MA 02138, USA

February 1, 2012

Abstract

The individual movements of large numbers of people are important in many contexts, from urban planning to disease spreading. Datasets that capture human mobility are now available and many interesting features have been discovered, including the ultra-slow spatial growth of individual mobility. However, the detailed substructures and spatiotemporal flows of mobility—the sets and sequences of visited locations—have not been well studied. We show that individual mobility is dominated by small groups of frequently visited, dynamically close locations, forming primary “habitats” capturing typical daily activity, along with subsidiary habitats representing additional travel. These habitats do not correspond to typical contexts such as home or work. The temporal evolution of mobility within habitats, which constitutes most motion, is universal across habitats and exhibits scaling patterns both distinct from all previous observations and unpredicted by current models. The delay to enter subsidiary habitats is a primary factor in the spatiotemporal growth of human travel. Interestingly, habitats correlate with non-mobility dynamics such as communication activity, implying that habitats may influence processes such as information spreading and revealing new connections between human mobility and social networks.

Understanding human movement is essential for a range of society-wide technological problems and policy issues, from urban planning [1] and traffic forecasting [2], to the modeling and simulation of epidemics [3, 4, 5]. Recent studies on mobility patterns have shown that spatiotemporal traces are highly non-random [6, 7, 8], exhibiting distinct dynamics subject to geographic constraints [9, 10, 11, 12, 13, 14]. Analytical models have been developed to reflect individual mobility dynamics such as the tendency to move back and forth between fixed locations on a regular basis [15]. When examining populations, movement patterns may be highly correlated with dynamics such as contact

preference [9, 11], yet this has not been well studied at the individual level. Previous work on human mobility has focused primarily on simple measures that forego the majority of the detailed information available in existing data. There is good reason for this, as basic approaches tend to be most fruitful for new problems. Yet these measures reduce an entire mobility pattern to a single scalar quantity, potentially missing important details and throwing away crucial information.

A number of approaches are available for studying the geographic substructure of individual mobility. One route is to perform spatial clustering [16] on the individual locations a user visits, potentially revealing important, related groups of locations. However, such analysis is purely spatial, neglecting the detailed spatiotemporal trajectories available for each user, reducing their mobility to a collection of geographic points and ignoring any information regarding the *flows*, or frequencies of movement, between particular locations. At the same time, the raw spatial distance separating two locations may not be meaningful: a short walk and a short car trip typically cover very different distances in the same amount of time, and the cognitive and economic costs associated with air travel depend only mildly (if at all) upon distance [17]. Modeling frameworks such as the Theory of Intervening Opportunities [18] and the recently introduced Radiation model [19] further argue that raw distances are not necessarily the most effective determinant for travel. In this work we show the importance of incorporating how frequently a user travels between two locations, which naturally accounts for spatial and dynamic effects while revealing the underlying spatiotemporal features of human mobility.

Results

Beginning from a country-wide mobile phone dataset [20, 7, 21, 8, 15, 22, 23, 24], we extract 34 weeks of call activity for a sample population of approximately 90 thousand users. Each call activity time series encodes the spatiotemporal trajectory of that phone user. (See Materials and Methods and Supporting Information (SI) for details about the data.) For each user we construct a directed, weighted *mobility network* capturing the detailed flows between individual locations (represented using cellular towers). Examples of both mobility networks and spatiotemporal mobility flows are shown in Figs. 1a and b, respectively. The recurrent and repetitive nature of human motion is clearly visible in Fig. 1b, where we explode the user trajectories vertically in time. We apply to each user's mobility network an information-theoretic graph partitioning method known as Infomap [25], which uses the flows of random walkers to find groups of dynamically related nodes in directed, weighted networks. We do not use spatial or distance information in partitioning, instead Infomap mirrors the stochastic process underlying human mobility flows; see SI Sec. 3 for details. (Infomap's underlying mechanism is further justified in this context by the results of [22].) The groups of locations that

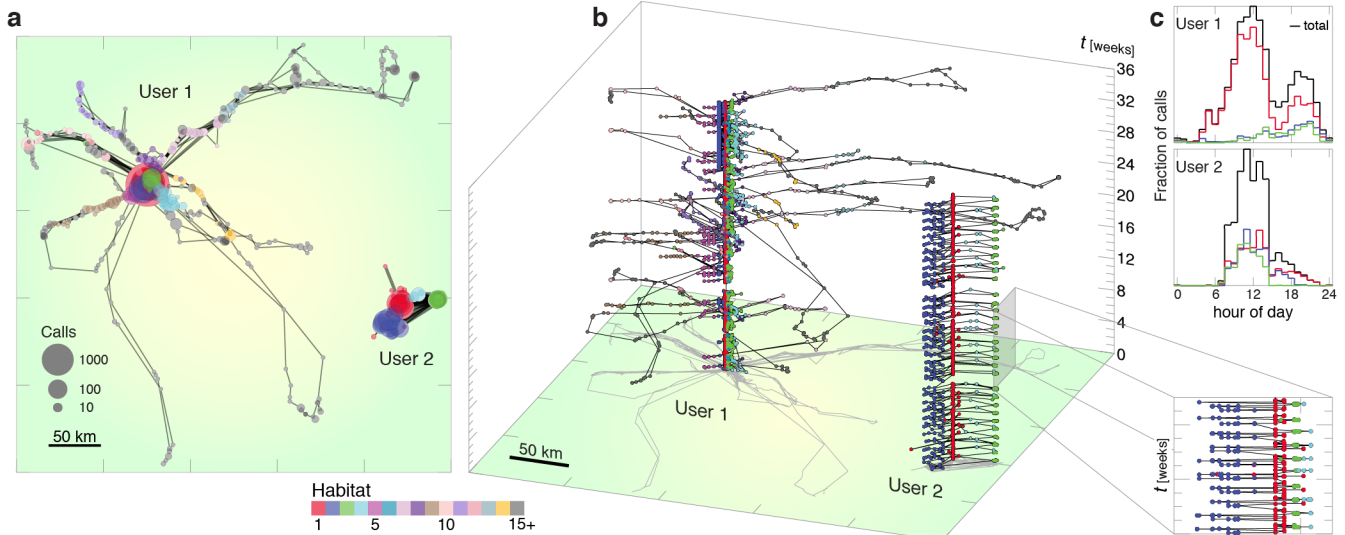


Figure 1: Habitats reveal the spatiotemporal substructure of human mobility patterns. **(a)** Spatial trajectories of two users, one traveling to a large number of locations and another covering a smaller range. Node size indicates the amount of time spent at a particular location (as quantified by mobile phone activity), node color represents the location’s habitat detected using Infomap (see Methods), and line width approximates the number of trips between locations. Habitats are ordered by call volume such that Habitat 1 contains the most calls. **(b)** Exploding the spatial trajectories from (a) in time (vertical axis), the recurrent nature of human mobility becomes evident, with a number of trips featuring both consistent destinations and consistently repetitive occurrence (zoom). These features are the root cause of the high predictability that human motion is known to possess. **(c)** The daily call dynamics of the three most active habitats, as well as the overall dynamics (summed over all habitats). The primary habitat contains the majority of temporal activity. We see that User 1 tends to occupy his or her second and third habitats primarily at night, while User 2 is more evenly distributed.

we discover, which we refer to as mobility “habitats,” will be shown to be crucial to both the spatiotemporal dynamics of human motion, and to the interplay between mobility and human interaction patterns. We rank habitats in decreasing order of phone activity, such that a user’s most frequently visited habitat is Habitat 1 or the primary habitat. We observe that human mobility is almost universally dominated by the primary habitat, where the majority of user call activity occurs—and thus it incorporates both home and work, home and school, or other major social contexts—along with a number of less active subsidiary habitats (see Fig. 1c and SI Sec. 3.2). These habitats, unique for each member of the population, differ greatly from existing work on partitioning mobility or social connectivity [26, 13, 27], which instead focus entirely on partitioning a single geographic network aggregated from large populations.

The spatial extent of a user’s total mobility pattern has been shown to be well summarized by a single scalar quantity, the radius of gyration, or gyradius, $R_g^2 = \langle |\mathbf{r}_i - \mathbf{r}_{CM}|^2 \rangle_i$, where \mathbf{r}_i is the spatial position of phone call i and \mathbf{r}_{CM} is the user’s center of mass [7]. In addition to using the global gyradius we also compute the reduced radius of gyration $r_g(h)$ for each habitat h , considering only those locations and calls contained within that habitat. In Fig. 2a we plot the population distributions of the first three habitat’s r_g , compared with the total gyradius R_g considering all

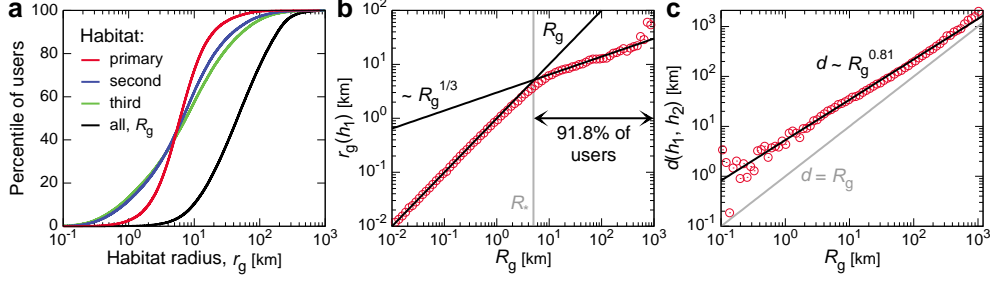


Figure 2: Spatial properties of mobility habitats. We characterize each habitat’s spatial extent by computing the radius of gyration $r_g(h)$ considering only calls placed from locations within habitat h . (a) The distribution of habitat radii over the population shows that the primary habitat tends to be more spatially compact than the less frequented habitats, though most are consistently smaller than the total R_g computed using all phone activity. Due to their heterogeneity, we characterize population distributions using percentiles, proportional to the cumulative distribution. (b) The growth in the radius of the primary habitat $r_g(h_1)$ as a function of total radius R_g . For $R_g < R_* \approx 5$ km, we see $r_g(h_1) \approx R_g$, indicating that those users are characterized by a single habitat. In contrast, $r_g(h_1) \sim R_g^{1/3}$ for $R_g > R_*$. Since approximately 92% of the population have $R_g > 5$ km, the majority of users exist in a regime where their primary habitat encompasses a potentially far smaller spatial region than their total mobility. (c) For users with multiple habitats, the distance $d(h_1, h_2)$ between the first and second habitat’s centers of mass is consistently greater than R_g (grey line) and exhibits power law scaling, $d(h_1, h_2) \sim R_g^\beta$, with $\beta = 0.81 \pm 0.02$. Taken together, we see that most habitats are both well separated and spatially compact, and that the magnitude of R_g is primarily due to movement between these habitats.

calls placed from all visited locations. This shows that the spatial extent of habitats tends to be far smaller than the total mobility, often by an order of magnitude, and that most users have a habitat r_g between 1–10 km. In Fig 2b we study the functional dependence of the primary habitat’s gyradius, $r_g(h_1)$, versus R_g . We uncover an intriguing power law scaling relation characterized by two regimes, where $r_g(h_1) \sim R_g^\alpha$ with $\alpha = 1$ for $R_g < R_* \approx 5$ km, and $\alpha = 1/3$ for $R_g > R_*$. The linear relationship below this critical radius size R_* indicates that most of those users (roughly 8% of the population) are exclusively characterized by a single habitat. But once a user’s range extends beyond this critical 5 km cutoff (true for 92% of the population) a new regime emerges where multiple habitats exist and tend to be far smaller and more spatially cohesive than the total mobility (since $\alpha < 1$). Finally, in Fig. 2c we show the geographic distance $d(h_1, h_2)$ between the centers of mass of the two most heavily occupied habitats, as a function of R_g . This also exhibits a power law scaling, $d(h_1, h_2) \sim R_g^\beta$ with $\beta = 0.81 \pm 0.02$. These distances tend to be far larger than the total R_g (grey line), indicating that the magnitude of R_g is primarily determined by movement between spatially cohesive and well separated habitats.

Given the importance of habitats to the spatial extent of human motion, one must ask: how do these habitats form and evolve over time? To what extent are the temporal dynamics of human movement reflected in the evolution of these habitats? Recently, considerable effort has been undertaken to understand the intriguing temporal features of human mobility, including the previously observed ultra-slow growth in time t of $R_g \sim (\log t)^\gamma$, with $\gamma > 1$ [7, 15]. Given the contribution of habitats to the magnitude of R_g , shown in Fig. 2, a primary question becomes: how do

habitats impact these temporal features? For example, how do individual habitat r_g 's evolve over time, compared with that of the total R_g ?

In Fig. 3 we study the temporal evolution of r_g and R_g by considering only those calls occurring up to time t , from either individual habitats or all locations, where $t = 0$ is the time of the user's first call. In Fig. 3a we plot the time series of $r_g(h_1)$ and R_g , normalized by the final values of each respective series. We observe that r_g saturates at its final value more quickly than the total mobility's R_g . To further quantify this saturation, we plot in Fig. 3b the ratio between $r_g(h_1)$ and R_g as a function of time, for groups of users with different final values of R_g . We observe increasingly rapid saturation of r_g as the total R_g increases. This implies that the primary habitat is explored more quickly than the total extent of a user's mobility pattern and that users who cover large distances explore their primary habitat more quickly relative to their total mobility than users who traverse relatively smaller regions. This is particularly interesting as one may initially expect such exploration to be at a constant rate relative to their total R_g . In Fig. 3c we study the temporal evolution of $r_g(t)$ for the first three habitats, averaged over users with $R_g \approx 30$ km. We observe approximately logarithmic growth, $r_g(h_1) \sim \log t$, for the primary habitat (slower growth than that observed in [7, 15]) while subsidiary habitats' gyradii $\sim (\log t)^\delta$, with $\delta > 1$ (growth more similar to [7, 15]). However, this analysis neglects an important detail: users do not begin exploring all of their habitats at the same time. Therefore in Fig. 3d we plot the same population-averaged radii, but we now individually shift each user's time series of $r_g(h)$ by a time $t_0(h)$, the time the user first entered habitat h , not simply made his or her first global call. Doing so accounts for the waiting times for users to visit habitats within our observation window. With this crucial correction we reveal *for all habitats* purely logarithmic growth in r_g , implying a universality in the exploration of habitats (which differ only in their overall spatial scale, with the primary habitat tending to be the most compact). Thus, the polylogarithmic growth of R_g , where R_g is initially small then grows faster than logarithmic in time, is primarily due to the temporal delay it takes users to exit their respective primary habitats and then rapidly traverse a relatively large distance to reach their other habitats.

Finally, a major question in the realm of mobility and human dynamics is the connection between spatiotemporal dynamics and other activity patterns [9]. For example, information spreading in heterogeneous systems of agents is a process that involves both the spatiotemporal mobility of the agents and their long-range communication activities. In this context, would the currently occupied habitat affect or be affected by how a user chooses a particular communication partner to engage? Such questions can also be addressed with mobile phone data, where phone communications capture a primary mode of information diffusion on the underlying social network [20]. To begin, we first recall a result from González et al. [7]. They found that users occupy locations following a Zipf law, where the probability $\Pr(L)$ to visit the L -th most frequented location follows $\Pr(L) \sim L^{-1.5}$. We reproduce this result in Fig. 4a. Interest-

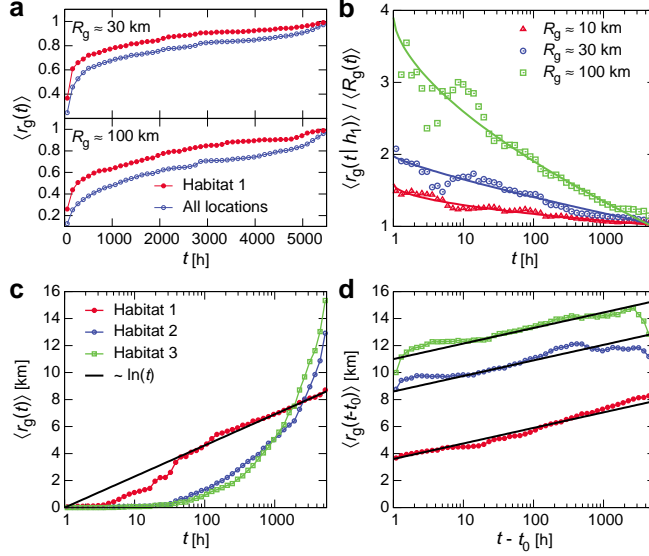


Figure 3: Temporal evolution of human mobility. **(a)** The time evolution of $r_g(h_1)$ compared with R_g , where both are normalized by their final values at the end of the observation window. We see that the primary habitat tends to reach saturation faster than the overall gyradius, indicating different temporal dynamics. **(b)** To quantify the saturation rate, we plot the ratio of the two curves from (a), for groups of users with different R_g . We see that the primary habitat saturates more quickly as the overall R_g grows. Solid lines of the form $\sim (\log t)^f$ provide a guide for the eye. **(c)** The unnormalized growth in habitat size for the first three habitats. The primary habitat shows a distinct, approximately logarithmic temporal scaling. The other habitats show a longer delay before r_g begins to grow polylogarithmically. **(d)** Given this delay, we now shift the time series of $r_g(h)$ for each habitat by $t_0(h)$, the time when the user first entered habitat h . Doing so we recover pure logarithmic scaling for all habitats, $r_g \sim \log(t - t_0)$, indicating that a major factor in the scaling of human mobility is the delay it takes for a user to transition to his or her non-primary habitats.

ingly, we discover (Fig. 4b) a potentially identical mechanism for how users choose to contact their communication partners, i.e. the probability $\text{Pr}(C)$ for a user to call his or her C -th most contacted partner also follows $\text{Pr}(C) \sim C^{-1.5}$. See also [28]. Finally, a number of the users within our population have contacts that are also within the population, meaning we have habitat information for both users. An interesting question is: how similar are the habitats of users in close communication, and will this similarity be lower for pairs with less frequent interaction? We measure the similarity between the primary habitats of pairs of users interacting with one another by computing the relative number of locations the habitats have in common (see Methods). In Fig. 4c we plot this Habitat similarity as a function of contact rank C . We see that, despite the Zipf law in Fig. 4b, users' primary habitats tend to be highly similar to the primary habitats of their most contacted ties. Nevertheless, there is little dependence on contact rank: one partner that is contacted an order of magnitude less often than another has almost the same primary habitat similarity. In other words, it takes very little communication to generate considerable habitat overlap [10]. Meanwhile, control habitats, generated by randomly distributing each user's visited locations between their habitats (see Methods), show smaller similarity and no effective trend.

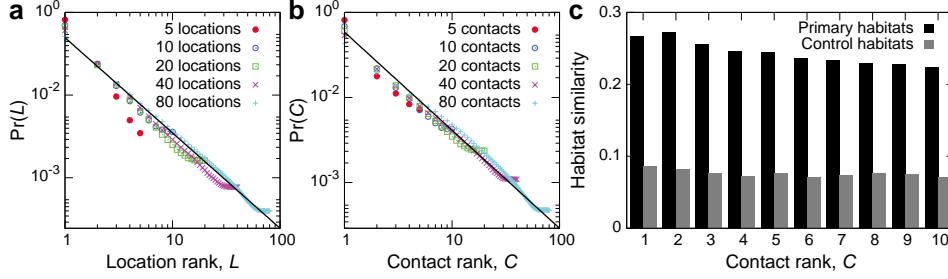


Figure 4: Contact activity and habitats. **(a)** The Zipf law governing the probability $\Pr(L)$ for a user to visit his or her L -th most visited location, as first observed by González et al. [7]. The solid line indicates $\Pr(L) \sim L^{-1.5}$ **(b)** Interestingly, we observe an identical Zipf law for the probability $\Pr(C) \sim C^{-1.5}$ for a user to call his or her C -th most contacted partner. This holds regardless of the total number of contacts for a user. This implies that the same underlying mechanism may govern how users choose both locations to visit and friends to contact. **(c)** The habitat similarity, related to the number of common locations, between a user’s primary habitat and the primary habitat of their contacts, averaged over pairs where both users are present in our data. We see that, despite the Zipf law in (b), users’ habitats tend to be surprisingly similar to their most contacted ties, even for those less frequently contacted users. Control habitats, generated by randomly shuffling a user’s visited locations between his or her original habitats, exhibit lower similarity. See Methods for habitat similarity and controls.

We further characterize the “interaction concentration” of a user by introducing P_{MFC} , the probability that the next call placed by the user goes to that user’s Most Frequent Contact, the partner that is most often in contact with the user. Users with a small P_{MFC} tend to distribute their calling activity more evenly across their partners, while users with large P_{MFC} are more concentrated and focus much of their attention upon a single individual. In Fig. 5 we study how P_{MFC} depends on the properties of a user’s mobility pattern. First, in Fig. 5a we show the distribution of P_{MFC} over the user population. Most users possess $0.1 \leq P_{\text{MFC}} \leq 0.4$ while very few users have either very small or very large P_{MFC} . In Fig. 5b we connect this interaction concentration with the user mobility patterns by showing that the mean P_{MFC} decays as the number of habitats a user visits grows. This means that users who travel broadly, leading to complex mobility patterns and multiple habitats, tend to distribute their communication activity more uniformly over their contacts. Finally, in Fig. 5c we quantify how P_{MFC} varies with the total gyradius R_g . We see an intriguing connection to a previous result: For users with small R_g , the P_{MFC} is small but grows as R_g grows. This continues until $R_g \approx R_*$, the same critical radius that appeared in Fig. 2b. Above R_* , we see that P_{MFC} now slowly decays with R_g . Since users with $R_g < R_*$ primarily possess a single habitat, these results imply that the mechanism governing how users distribute their activity over their contacted partners may differ for those users who primarily possess a single habitat compared with those users whose mobility leads to multiple habitats. We used Kendall rank correlation and associated hypothesis tests [29] to verify the statistical validity of the observed relationships. See SI Sec. 6 for hypothesis tests between these and additional measures.

The mobile phone data also provides demographic information for the majority of users, specifically self-reported

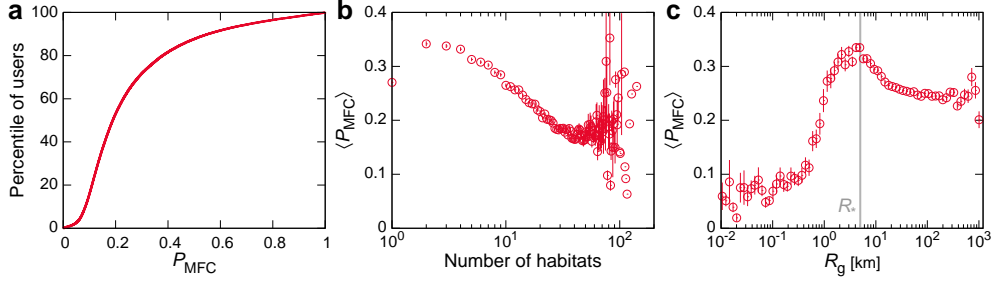


Figure 5: Communication and mobility dynamics. We characterize the interaction concentration of a user by P_{MFC} , the probability for that user to place a call to his or her Most Frequent Contact. (a) The distribution of P_{MFC} over the population shows that most users have P_{MFC} between approximately 0.1 and 0.4. (See also Fig. 4b.) (b) To connect the concentration with user mobility, we study how the mean P_{MFC} varies with the number of habitats each user possesses. We see that P_{MFC} gradually decays as the number of habitats grows, indicating that broadly traveled individuals tend to more evenly distribute their calls over their partners. (c) Studying P_{MFC} as a function of R_g , we uncover an intriguing relationship. For users with particularly small mobility ranges, P_{MFC} is small but grows as R_g grows. This continues until $R_g \approx R_*$, the same critical radius size observed in Fig. 2b. The mean P_{MFC} then decays for $R_g > R_*$. Surprisingly, this implies that the distribution of call activity over a user’s partners exhibits different behavior depending on whether that user possess one mobility habitat, or many habitats. Error bars in b and c indicate ± 1 s.e.

age and gender. In SI Sec. 4 we study the results of Fig. 5 after decomposing the sample into age and gender groups. One may expect these results to change when focusing on these different groups. Yet we find qualitatively similar results to Fig. 5 with only small differences: P_{MFC} tends to be slightly higher for women than for men, and increases with user age. After considering these demographic dependencies on P_{MFC} , we observe the same relationships between communication activity and mobility.

Discussion

We have shown that accurately understanding human mobility requires an analysis using the complete spatiotemporal flows captured for each user. Basic measures such as the gyradius R_g constitute an excellent starting point, but such single scalar quantities simply cannot capture the full complexity of an individual mobility pattern. As the quality and quantity of available data increases, we expect our understanding of the various factors shaping human mobility to continue to improve.

Given that users spend the majority of time occupying their primary habitats, understanding the detailed features of the primary habitat will be crucial for applications such as search and rescue during emergencies [23] or containing the spread of epidemic diseases [3, 4, 5], since most users will be within their primary habitats at the onset of such events. Meanwhile, detailed information regarding unusual trips away from the primary habitat may prove useful both for curtailing diseases and for optimizing transportation infrastructure and energy usage. Likewise, the purely

logarithmic scaling laws for intra-habitat mobility uncovered in Fig. 3d are not accounted for by current modeling frameworks [15]; more effort may be necessary to acceptably model the microscopic structure of individual human motion. The connections we reveal between communication dynamics and human mobility may have important consequences for understanding the spread of information or rumors through a population, as such processes may spread both spatially and socially [30]. Further investigation of such connections may prove fruitful in a number of areas, including information diffusion and social contagion.

Methods

Dataset

We use a large-scale, de-identified mobile phone dataset, previously studied in [20, 7, 21, 8, 15, 22, 23]. We sample approximately 90 thousand users from the total dataset, according to the activity criteria introduced in [8]. We retain nine months of phone activity for each user. A “call” is either a text message or a voice call, and we use the cellular tower that handled the communication to represent the location $L(t)$ of a call made at time t . Call times are kept at an hourly resolution. The coordinates of these towers are used to compute the radii of gyration [7]. Phone call recipients determine the communication partners of a user. Since a single phone call between two individuals may not represent a meaningful tie, we consider user B to be a partner of user A only if we observe at least one reciprocated pair of calls (A called B and B called A) [20]. We do not require user B to be in our sample population, except when we compute habitat similarity.

Finding mobility habitats

For each user we convert their trajectory $\xi = \{L(t_1), L(t_2), \dots\}$, with $t_i > t_{i'}$ for $i > i'$, into a weighted digraph where the weight on link $L_i \rightarrow L_j$ represents the number of times the ordered pair of locations (L_i, L_j) was observed in ξ . The community discovery method Infomap [25] was applied to each digraph, using the default parameters (10 attempts and self-loops ignored). The discovered groups of locations are the habitats for that user. Habitats are ranked by total number of calls.

Habitat similarity

For a user A with contact B , both present in our sample, we define the similarity $S(A, B)$ between their primary habitats to be the Jaccard coefficient between the sets of locations comprising those habitats. If these sets are disjoint

$S(A, B) = 0$, whereas $S(A, B) = 1$ if they overlap completely.

Controls

It is important to understand the significance of the results we have presented here, in particular whether the results associated with the habitats we find are meaningful. We compute null or control habitats, generated for each user, by randomly assigning that user's visited locations to habitats while preserving the number of habitats and the number of locations within each habitat. This strictly controls for the habitat size distributions while testing the effects of habitat membership. In Fig. S6 we further show that the pure logarithmic time evolution is absent in control habitats, indicating that the temporal evolution we observe in Fig. 3d is not due to the relative sizes (numbers of locations) of the habitats, nor to simply the number of habitats, but due more fundamentally to their spatial structure and the spatiotemporal flows of the users. In Fig. 4 we see that these control habitats have lower similarity than the actual habitats. See SI Sec. 6 for details.

Acknowledgments

We thank F. Simini, J. Menche, J.-P. Onnela, S. Lehmann, W.-T. Chung, D. Brockmann, B. Uzzi, and D. Lazer for many useful discussions and A.-L. Barabási, D. Lazer, B. Uzzi and D. Brockmann for support. The authors gratefully acknowledge the Center for Complex Network Research, supported by the James S. McDonnell Foundation 21st Century Initiative in Studying Complex Systems, NSF within the Information Technology Research (DMR-0426737) and IIS-0513650 programs, the Defense Threat Reduction Agency award HDTRA1-08-1-0027 and HDTRA1-10-1-0100, the Network Science Collaborative Technology Alliance sponsored by the U.S. Army Research Laboratory under agreement number W911NF-09-2-0053, and the U.S. Office of Naval Research Award (N000141010968).

References

- [1] M.W. Horner and M.E. O'Kelly. Embedding economies of scale concepts for hub network design. *Journal of Transport Geography*, 9(4):255–265, 2001.
- [2] R. Kitamura, C. Chen, R. M. Pendyala, and R. Narayanan. Micro-simulation of daily activity-travel patterns for travel demand forecasting. *Transportation*, 27(1):25–51, 2000.
- [3] R. Pastor-Satorras and A. Vespignani. Epidemic spreading in scale-free networks. *Physical review letters*, 86(14):3200–3203, 2001.
- [4] L. Hufnagel, D. Brockmann, and T. Geisel. Forecast and control of epidemics in a globalized world. *Proceedings of the National Academy of Sciences of the United States of America*, 101(42):15124, 2004.

- [5] V. Colizza, A. Barrat, M. Barthélemy, and A. Vespignani. The role of the airline transportation network in the prediction and predictability of global epidemics. *Proceedings of the National Academy of Sciences of the United States of America*, 103(7):2015, 2006.
- [6] D. Brockmann, L. Hufnagel, and T. Geisel. The scaling laws of human travel. *Nature*, 439(7075):462–465, 2006.
- [7] M. C. González, C. A. Hidalgo, and A.-L. Barabási. Understanding individual human mobility patterns. *Nature*, 453(7196):779–782, 2008.
- [8] C. Song, Z. Qu, N. Blumm, and A.-L. Barabási. Limits of predictability in human mobility. *Science*, 327(5968):1018, 2010.
- [9] N. Eagle, A. S. Pentland, and D. Lazer. Inferring friendship network structure by using mobile phone data. *Proceedings of the National Academy of Sciences*, 106(36):15274, 2009.
- [10] D. J. Crandall, L. Backstrom, D. Cosley, S. Suri, D. Huttenlocher, and J. Kleinberg. Inferring social ties from geographic coincidences. *Proceedings of the National Academy of Sciences*, 107(52):22436, 2010.
- [11] D. Wang, D. Pedreschi, C. Song, F. Giannotti, and A.-L. Barabási. Human mobility, social ties, and link prediction. In Chid Apté, Joydeep Ghosh, and Padhraic Smyth, editors, *KDD*, pages 1100–1108. ACM, 2011.
- [12] F. Calabrese, Z. Smoreda, V. D. Blondel, and C. Ratti. Interplay between telecommunications and face-to-face interactions: A study using mobile phone data. *PLoS ONE*, 6(7):e20814, 07 2011.
- [13] P. Expert, T. S. Evans, V. D. Blondel, and R. Lambiotte. Uncovering space-independent communities in spatial networks. *Proceedings of the National Academy of Sciences*, 108(19):7663, 2011.
- [14] P. Hui, A. Chaintreau, J. Scott, R. Gass, J. Crowcroft, and C. Diot. Pocket switched networks and human mobility in conference environments. In *Proceedings of the 2005 ACM SIGCOMM workshop on Delay-tolerant networking*, pages 244–251. ACM, 2005.
- [15] C. Song, T. Koren, P. Wang, and A.-L. Barabási. Modelling the scaling properties of human mobility. *Nature Physics*, 2010.
- [16] A. K. Jain, M. N. Murty, and P. J. Flynn. Data clustering: a review. *ACM computing surveys (CSUR)*, 31(3):264–323, 1999.
- [17] M. Brons, E. Pels, P. Nijkamp, and P. Rietveld. Price elasticities of demand for passenger air travel: a meta-analysis. *Journal of Air Transport Management*, 8(3):165–175, 2002.
- [18] S. A. Stouffer. Intervening opportunities: a theory relating mobility and distance. *American sociological review*, 5(6):845–867, 1940.
- [19] F. Simini, M. C. González, A. Maritan, and A.-L. Barabási. A universal model for mobility and migration patterns. *Nature*, 2012 (to appear). arXiv:1111.0586.
- [20] J.-P. Onnela, J. Saramäki, J. Hyvönen, G. Szabó, D. Lazer, K. Kaski, J. Kertész, and A.-L. Barabási. Structure and tie strengths in mobile communication networks. *Proceedings of the National Academy of Sciences*, 104(18):7332, 2007.
- [21] J. P. Bagrow and T. Koren. Investigating bimodal clustering in human mobility. In *International Conference on Computational Science and Engineering, 2009. CSE'09.*, volume 4, pages 944–947. IEEE, 2009.
- [22] J. Park, D.-S. Lee, and M. C. González. The eigenmode analysis of human motion. *Journal of Statistical Mechanics: Theory and Experiment*, 2010:P11021, 2010.
- [23] J. P. Bagrow, D. Wang, and A.-L. Barabási. Collective response of human populations to large-scale emergencies. *PLoS ONE*, 6(3):e17680, 03 2011.

- [24] J.-P. Onnela, S. Arbesman, M. C. González, A.-L. Barabási, and N. A. Christakis. Geographic constraints on social network groups. *PLoS ONE*, 6(4):e16939, 04 2011.
- [25] M. Rosvall and C. T. Bergstrom. Maps of random walks on complex networks reveal community structure. *Proceedings of the National Academy of Sciences*, 105(4):1118, 2008.
- [26] C. Thiemann, F. Theis, D. Grady, R. Brune, and D. Brockmann. The structure of borders in a small world. *PLoS ONE*, 5(11):e15422, 11 2010.
- [27] C. Ratti, S. Sobolevsky, F. Calabrese, C. Andris, J. Reades, M. Martino, R. Claxton, and S. H. Strogatz. Redrawing the map of great britain from a network of human interactions. *PLoS ONE*, 5(12):e14248, 12 2010.
- [28] L. Backstrom, E. Bakshy, J. Kleinberg, T. M. Lento, and I. Rosenn. Center of attention: How facebook users allocate attention across friends. In *Proc. 5th International Conference on Weblogs and Social Media*, 2011.
- [29] M. Kendall and J. D. Gibbons. *Rank Correlation Methods*. C. Griffin, 5th edition, 1990.
- [30] J. M. Kleinberg. Navigation in a small world. *Nature*, 406(6798):845–845, 2000.

Supporting Information

Spatiotemporal features of human mobility

by James P. Bagrow and Yu-Ru Lin

Table of Contents

S1 Dataset	13
S2 Mobility networks	14
S3 Mobility habitats	14
S3.1 Justification for Infomap	15
S3.2 Additional properties of mobility habitats	15
S4 Demographic and communication effects	16
S5 Data sparsity	17
S6 Controls and hypothesis tests	18
References	20

List of Figures

S6 Properties of mobility networks.	14
S7 Additional habitat statistics	15
S8 Habitat gyradius versus habitat rank	16
S9 Population distributions of habitat arrival times	16
S10 Demographics and extensions of interaction concentration	17
S11 Missing data do not affect most statistics	18
S12 Temporal evolution of gyradius for real and null habitats	19

List of Tables

S1 Nonparametric correlations between mobility and communication	19
--	----

S1 Dataset

We use a set of de-identified billing records from a Western European mobile phone service provider [1, 2, 3, 4, 5, 6]. The records cover approximately 10M subscribers within a single country over 3 years of activity. Each billing record, for voice and text services, contains the unique identifiers of the caller placing the call and the callee receiving the call; an identifier for the cellular antenna (tower) that handled the call; and the date and time when the call was placed. Coupled with a dataset describing the locations (latitude and longitude) of cellular towers, we have the approximate location of the caller when placing the call. For this work we do not distinguish between voice calls and text messages, and refer to either communication type as a “call.”

These phone records cover approximately 20% of the country’s mobile phone market. However, we also possess identification numbers for phones that are outside the service provider but that make or receive calls to users within the company. While we do not possess any other information about these lines, nor anything about their users or calls that are made to other numbers outside the service provider, we do have records pertaining to all calls placed to or from those ID numbers involving subscribers covered by our dataset. Thus egocentric networks [7] between users within the company and their immediate neighbors only are complete. This information was used to generate egocentric communication networks and to study the MFC probability and its relationship to human mobility patterns.

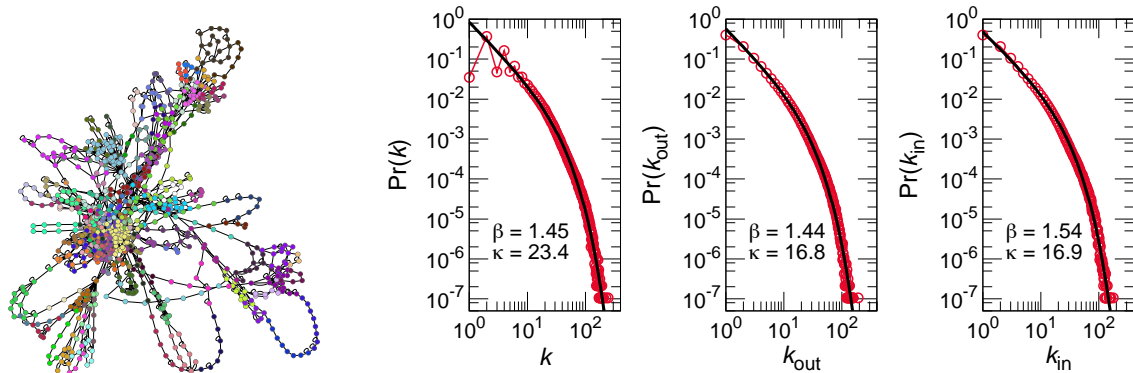


Figure S6: **Properties of mobility networks.** (a) An example mobility network (MobNet), drawn without using spatial coordinates. Several dense cores are visible, as are a number of unusually long loops, representing one-time trips. Node colors indicate habitats, discovered using Infomap [9]. Link weights and directions have been omitted for clarity. (b) Degree distributions (undirected, outdegree, and indegree) for all MobNets. All are well described by a power law with an exponential cutoff, $\Pr(k) \sim k^{-\beta} e^{-k/\kappa}$, meaning that users typically visit many locations only a small number of times while a few locations are visited many times. Note that here “degree” refers to the number of connections per location (the number of unique locations visited before or after visiting that location) not the number of communication partners a user has.

We generate a sample population of approximately 90k users (specifically, $N = 88137$), using the criteria introduced in [3]. Each user’s call history during our nine-month tracking period yields three time series: (i) event times for when calls are made, kept to an hourly resolution; (ii) locations of calls, as quantified by the cellular tower transmitting the call; and (iii) communication partners who receive calls. These time series allow us to reconstruct both geographic trajectories and egocentric communication networks for each user.

S2 Mobility networks

We construct for each sample user a weighted, directed mobility network G (or *MobNet* for short) using the user’s time-ordered trajectory $\{L(t_1), L(t_2), \dots\}$, where $L(t)$ is the location the user called from at time t . Each link ($L_i \rightarrow L_j$) in G represents the user placing a call at location L_i followed by a call at location L_j . The weight on link ($L_i \rightarrow L_j$) gives the number of times the user made that particular relocation during the sample window.

In Fig. S6a we draw the mobility network of a single user. This network was drawn using a typical force-directed graph layout algorithm [8] and does not use geographic tower locations. We see several dense cores comprising groups of frequently visited locations as well as a number of long loops or chains representing sequential calls placed during one-time, typically long-range trips. These mobility networks feature broad degree distributions, well described by a truncated power law of the form $\Pr(k) \sim k^{-\beta} e^{-k/\kappa}$, for constants β and κ , where k is the number of connections of a location (or number of unique locations visited before or after visiting that location). The nature of this broad distribution is not surprising given the Zipf law for location selections, observed in [2] (see also Main text Fig. 4a). Although one may not expect this distribution to hold for both in- and out-degrees, we do observe similar patterns in our directed networks.

S3 Mobility habitats

In this work we start by identifying groups of related locations, for each user. These groups may correspond to home, work, school, or any number of other contexts throughout daily life. The mobility networks we study are inherently spatial, possessing a unique geographical embedding, yet we do not discover these groups through spatial clustering methods, so it may be misleading to refer to these groups as clusters. Likewise, although we use a community detection method known as Infomap [9] to find these groups, mobility networks are not social networks, so referring to these groups as communities may also be misleading. To avoid confusion, we instead term these groups “habitats.” We rank each user’s habitats by the total number of phone calls that occur within the habitat, so that Habitat 1 is most active,

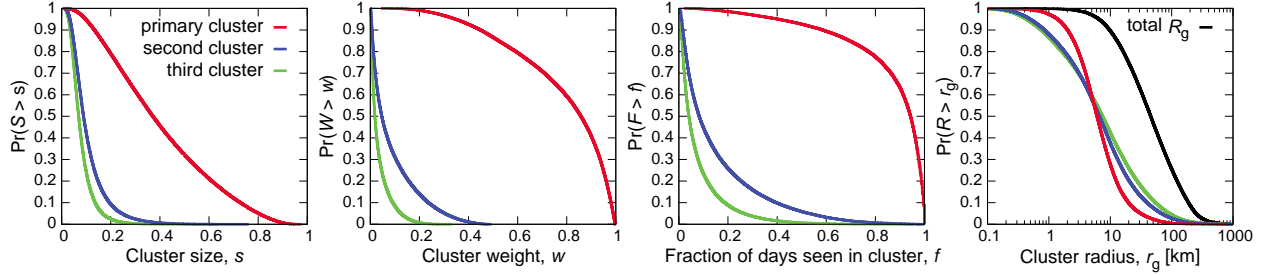


Figure S7: **Additional habitat statistics.** We plot the complementary cumulative distributions of habitat size (number of unique locations within the habitat), habitat weight (number of calls placed from within the habitat), the fraction of days during the nine-month window where the user was active and was observed in the habitat, and the habitat radius of gyration. The gyration distributions were also shown in main text Fig. 2a. We see that the primary habitat occupies most locations, the majority of phone activity, and that most users are found in the habitat nearly every day. Thus the primary habitat captures the majority of user dynamics.

Habitat 2 is second most active, etc. Habitats are not ranked by number of locations, though these tend to correlate. See Methods and materials in the main text for details on how to apply Infomap.

S3.1 Justification for Infomap

There are numerous algorithms for detecting communities in networks [10]. We believe Infomap to be ideally suited for our purposes here, for two main reasons. The first reason is that it is specifically capable of handling both weighted and directed networks, and much of the focus of the original publication [9] was devoted to the sometimes confusing effects of community structure in directed networks. Infomap’s theoretical basis rests upon the notion of random walkers moving through the network. These walkers can readily adapt to link weights and link directions, no modifications to the underlying algorithm are necessary.

The second reason for adopting Infomap relates to a result from Park, Lee, and González [11]. They present the at-first-glance paradoxical result that a random walk model on an empirically-derived mobility network does well at reproducing macroscopic phenomena, such as the gyradius. This seems surprising given that human beings have long-term memory, and consistently travel between fixed sets of destinations [2], unlike a diffusing random walker. Even in [3] it was shown, using estimates of the Kolmogorov entropy of a human trajectory, that there is more information in a trajectory than estimated by the Shannon entropy alone. (The resolution of this paradox is to note that a random walker exploring a new space of locations will not be able to *generate* mobility networks such as those we derive from the mobile phone data; a more complex modeling framework is necessary [4].) Thus, while there is information in a human trajectory beyond the mobility network, the mobility network still captures a great deal of mobility phenomena. Infomap’s theoretical basis exactly matches this random-walker-on-a-mobility-network model.

S3.2 Additional properties of mobility habitats

We remark on several additional features of mobility habitats not fully discussed in the main text. In Fig. S7 we plot the distributions over the sampled user population of several quantities of interest for the habitats. These are the “size” of each habitat, as given by the number of unique locations within the habitat; the “weight” of each habitat, given by the number of phone calls placed from locations within the habitat; the fraction of days during the nine-month sample window where the user was active making calls and observed in the habitat; and the distribution of habitat spatial extent, given by the gyradius. We see that the primary habitat tends to contain most locations and the overwhelming majority of call activity, and that many users appear in their primary habitat almost every day. Thus the primary habitat tends to capture the intrinsic or typical day-to-day activity of a user.

Another feature we study here is the spatial extent of habitat h , captured by its gyradius $r_g(h)$, as a function of the rank h of the habitat. We show in Fig. S8 that more active (lower h) habitats tend to be smaller on average, going from $r_g \approx 10$ km to $r_g \approx 20$ km as h goes from 1 to 3. However, we see a rapid saturation in r_g to values typically between

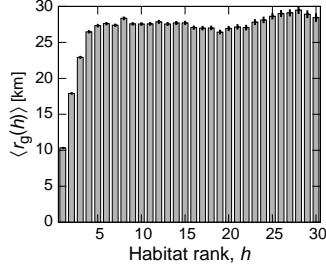


Figure S8: **Habitat gyradius versus habitat rank.** We see that the most active habitats tend to be more compact spatially, on average, than those less frequented habitats. The overall habitat size quickly saturates at around 25 – 30km, however, indicating an intrinsic maximum spatial extent. Error bars represent ± 1 s.e.

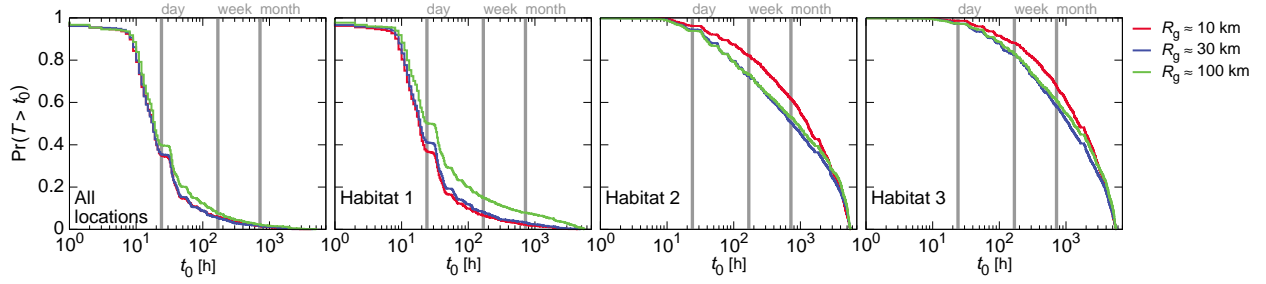


Figure S9: **Population distributions of habitat arrival times.** The distributions of times t_0 when each user placed his or her first call from any location or from within a habitat. Different curves represent groups of users with different total gyradius R_g . We see that most users place their first call within Habitat 1 very early, often within a day of the start of data collection. As R_g grows, these distributions change only slightly, with far ranging travelers having a slightly higher probability of delaying their first appearance in Habitat 1 (green curve). Habitats 2 and 3 show longer waits until users arrive at these locations. Interestingly, there is only a minor dependence on R_g : users with smaller values of R_g (red curve) tend to wait slightly longer to enter these habitats.

25 to 30 km, for $h > 5$. This indicates that there is an **intrinsic upper bound** on effective habitat spatial extent, further emphasizing their cohesive nature.

Finally, we also study the distribution of habitat entrance times $t_0(h)$, the time it takes for the user to first enter a location within habitat h ($t = 0$ is the time of the user’s first call). In the main text we show how the delay in entering habitats greatly alters the temporal scaling in r_g , so that habitats grow only logarithmically in time, distinct from the polylogarithmic growth reported in the literature for the full mobility pattern [2, 4]. We present in Fig. S9 the complementary cumulative distributions of t_0 for the first three habitats, as well as the time it takes for the first call to occur (which can be thought of as t_0 for all locations). We see that the distribution for Habitat 1 is functionally similar to the total distribution, while t_0 for Habitats 2 and 3 tends to be higher in value. We see a minor dependence on the total mobility extent, quantified with R_g : Users with higher R_g tend to wait longer before entering Habitat 1, perhaps because they are more likely to be traveling far from home when data collection begins, while users with lower R_g tend to wait slightly longer before entering Habitats 2 or 3, perhaps because they tend to travel less frequently. These results further emphasize the fundamental role that mobility habitats play in determining the magnitude and dynamics of human mobility and travel patterns.

S4 Demographic and communication effects

We decompose the sample population by self-reported age and gender, and present the results from main text Fig. 5 with respect to different age and gender groups. Results for the different groups are shown in Fig. S10a and S10b. We see the same overall features for these groups, with some small quantitative differences, that we observed in the main text for the entire population. We also compare in Fig. S10c the probability of calling the most frequent contact (P_{MFC}) with the cumulative probabilities of calling the top-two and top-three most frequently contacted communication partners. We see that the cumulative probabilities exhibit a similar trend as P_{MFC} with respect to mobility, suggesting that the relationship between mobility patterns and interaction concentration captured by P_{MFC} is stable over the most

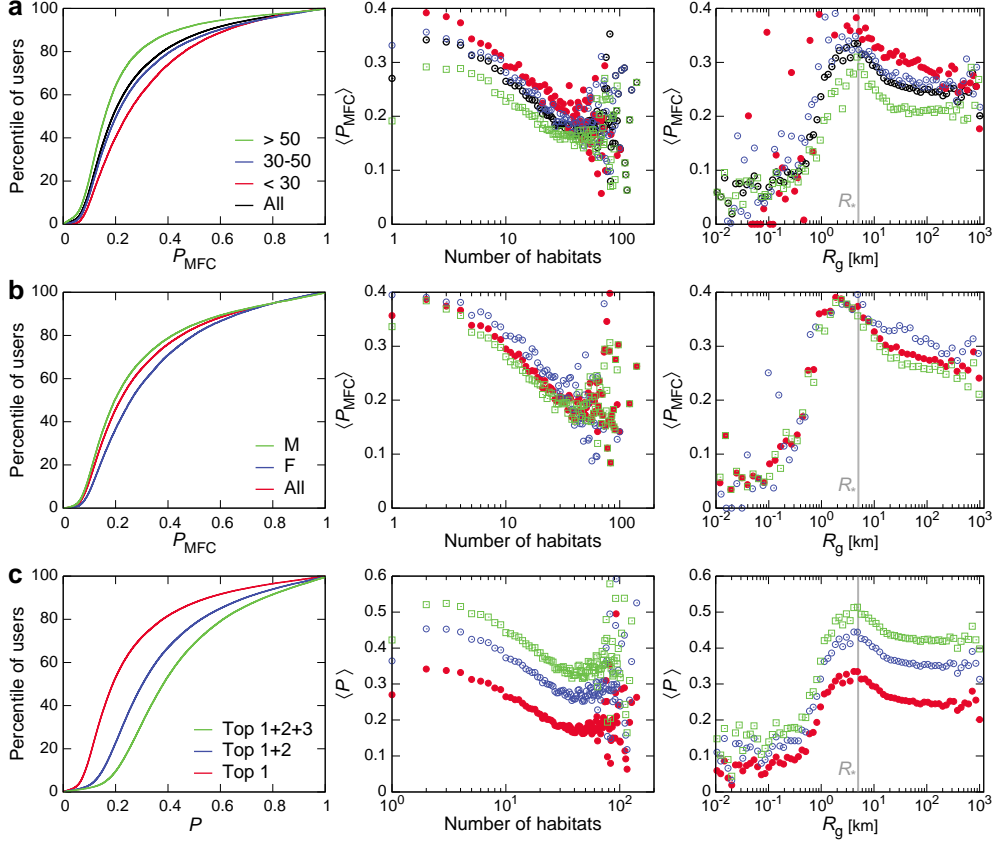


Figure S10: **Demographics and extensions of interaction concentration.** (a) Age groups. Users older than fifty tend to be less concentrated on their MFC, while younger generations focus more on their MFC. (“All” indicates all users with self-reported age.) (b) Gender groups. Female users call slightly more to their MFC than male users. (“All” indicates all users with self-reported gender.) (c) The cumulative probabilities for calling the top-two and top-three most frequently contacted friends exhibit similar trends as P_{MFC} with respect to the mobility measures. Overall, the primary difference for the demographic groups is the average value of their respective P_{MFC} . After accounting for this, we observe the same relationships between P_{MFC} and mobility.

frequently contacted partners.

S5 Data sparsity

There is an important factor to consider when using mobile phone data and that is how phone usage affects measurements, as data are available only when users engage their mobile phones. While we select active users using the criteria of [3], specifically intended to mitigate such problems, there still exist many time periods where a user does not use the phone and thus we do not have any information. We now study this in further detail.

We compute for each user the fraction of hours q , out of the nine-month window, where the user is not active. In Fig. S11 we plot the distribution of q over the 90k users; we see that users are inactive on average around 75% of the time. (This distribution, and its consequences, was also discussed in [3].) While this may seem problematic at first, we are able to proceed because we are integrating over such a long time window, extracting robust amounts of data for the quantities we are interested in. For example, in Fig. S11 we also plot the number of communication partners k , the distance between the first and second habitats $d(h_1, h_2)$, and the total gyradius R_g , all as a function of the missing fraction q . We see almost no trend or dependence on q . Meaning that users missing data 40% of the time give the same or similar statistics as users missing data 80% of the time, for example. Only for the gyradius do we see a small drop in R_g for larger values of q . We note, however, that even this trend remains within 1 s.d. and is thus not significant.

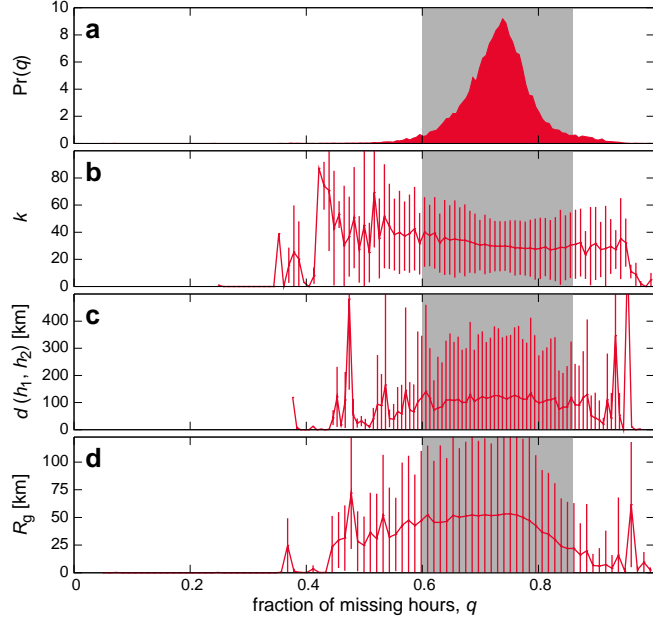


Figure S11: **Missing data do not affect most statistics.** Mobile phone data is inherently incomplete since data is only available when users place calls. We apply the selection criteria used in [3] to mitigate the missing data issue. When considering the fraction of hours q without data out of the 34 weeks, we see that users are typically missing data $\approx 75\%$ of the time (a). One may expect this to cause bias, yet for a number of measures (b–d) we see almost no trend in the shaded region (containing $\approx 95\%$ of the population). Only for the gyradius (d) do we see a minor dependence for higher values of q . These results indicate that our measures are not sensitive to missing data. Error bars indicate ± 1 s.d.

S6 Controls and hypothesis tests

We introduce Habitat controls to determine how meaningful the discovered habitats are, where we use different groupings of mobility locations to form control or null habitats. To compute habitat controls we form randomized habitats by shuffling locations between the original habitats at random in such a way as to preserve for each user both the number of habitats and the number of locations per habitat, strictly controlling for the size distributions of the habitats. These control for the nature of the groupings we find and whether or not it is meaningful for particular locations to share a habitat.

To begin, in Fig. S12a-c we show the temporal evolution of the gyradius $r_g(t)$ vs. t for the first three habitats. We study three sets of users, with total $R_g \approx 10, 30,$ and 100 km, respectively. For all groups we see that $r_g \sim \log(t - t_0)$, amplifying the results from main text Fig. 3d. Meanwhile, in Fig. S12d-f we show the same quantities but for the shuffled habitats where locations are randomized. We see that the pure logarithmic time evolution is lost, indicating that the evolution we observe is not due to the relative sizes (numbers of locations) of the habitats, nor to simply the number of habitats, but due more fundamentally to their spatial structure and the spatiotemporal flows of the users.

Meanwhile, the results from main text Fig. 5 show an intriguing relationship between human mobility and communication activity. Here we quantify the relationship using the Kendall’s τ (tau-b) rank correlation coefficient [12], which is a nonparametric hypothesis test used to measure the association between two measured quantities. The coefficient $\tau > 0$ indicates positive association, $\tau < 0$ indicates negative association, and $\tau = 0$ indicates the absence of association.

Mobility is evaluated by the number of habitats N_H and the total gyradius R_g , while interaction concentration is quantified by the probability of calling the most frequent contact P_{MFC} , the cumulative probability of calling the top-three most frequently contacted partners C_{MFC} , and the total number of partners k .

In Table S1, we see a negative association between N_H and P_{MFC} (as well as C_{MFC}), while N_H and k are positively correlated. This suggests that people who are more habitually mobile (with more habitats) tend to distribute their communication over more contacted ties.

An association between R_g and the communication measures at first appears absent. However, when separating users who possess only a single habitat ($N_H = 1$) from those who don’t ($N_H > 1$), we discover that the relationship with R_g shows two opposing trends: for users with a single habitat, R_g grows with P_{MFC} ; when users have more than one habitat, their P_{MFC} begin to drop. These correlations suggest a coupling between mobility habitats and interaction concentration, which cannot be captured by a single R_g value.

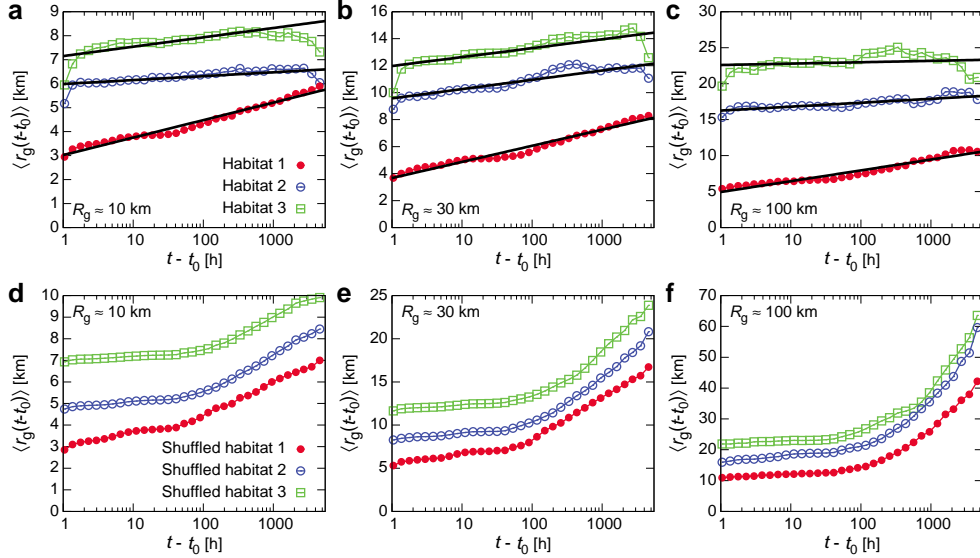


Figure S12: **Temporal evolution of gyradius for real and null habitats.** (a-c) Real habitats. The temporal evolution of $\langle r_g(h) \rangle \sim \log(t - t_0)$ in all cases for user groups with total $R_g \approx 10, 30$, and 100 km. Straight lines indicate fits of the form $r_g = A \log(t - t_0) + B$, for constants A and B . (d-f) Null habitats. The same as a-c but for randomized control habitats, constructed for each user by randomly reshuffling locations between habitats while preserving the number of habitats and the number of locations within each habitat. We see the pure logarithmic scaling of r_g is lost.

Table S1: **Nonparametric correlations between mobility and communication.** We quantify the relationship between mobility (columns) and communication (rows) using Kendall's τ rank correlation coefficient. User mobility is evaluated by the number of habitats N_H and the gyradius R_g , and their concentration is evaluated by P_{MFC} , C_{MFC} (the cumulative probability of calling any of the three most frequently contacted partners) and k (the number of partners). Each table entry shows the coefficient τ and its corresponding p -value (parenthesis). We see a negative association between N_H and P_{MFC} (and C_{MFC}), while N_H and k are positively correlated. An association between R_g and the communication measures appears absent. However, when separating users with a single habitat ($N_H = 1$) from the rest ($N_H > 1$), we see that the growth of R_g has two opposite trends: within a single habitat, R_g grows with P_{MFC} ; when users have more than one habitat, P_{MFC} begin to drop. This implies a coupling between mobility habitats and interaction concentration, one that cannot be captured by R_g alone.

Communication	Mobility			
	N_H	R_g	$R_g (N_H = 1)$	$R_g (N_H > 1)$
P_{MFC}	-0.133 ($< 2.2 \times 10^{-16}$)	-0.00648 (0.0039)	0.354 ($< 2.2 \times 10^{-16}$)	-0.0324 ($< 2.2 \times 10^{-16}$)
C_{MFC}	-0.153 ($< 2.2 \times 10^{-16}$)	-0.0127 (1.7×10^{-8})	0.358 ($< 2.2 \times 10^{-16}$)	-0.0369 ($< 2.2 \times 10^{-16}$)
k	0.214 ($< 2.2 \times 10^{-16}$)	-0.0728 ($< 2.2 \times 10^{-16}$)	-0.44 ($< 2.2 \times 10^{-16}$)	-0.0619 ($< 2.2 \times 10^{-16}$)

References

- [1] J.-P. Onnela, J. Saramäki, J. Hyvönen, G. Szabó, D. Lazer, K. Kaski, J. Kertész, and A.-L. Barabási. Structure and tie strengths in mobile communication networks. *Proceedings of the National Academy of Sciences*, 104(18):7332, 2007.
- [2] M. C. González, C. A. Hidalgo, and A.-L. Barabási. Understanding individual human mobility patterns. *Nature*, 453(7196):779–782, 2008.
- [3] C. Song, Z. Qu, N. Blumm, and A.-L. Barabási. Limits of predictability in human mobility. *Science*, 327(5968):1018, 2010.
- [4] C. Song, T. Koren, P. Wang, and A.-L. Barabási. Modelling the scaling properties of human mobility. *Nature Physics*, 2010.
- [5] J. P. Bagrow and T. Koren. Investigating bimodal clustering in human mobility. In *International Conference on Computational Science and Engineering, 2009. CSE'09.*, volume 4, pages 944–947. IEEE, 2009.
- [6] J. P. Bagrow, D. Wang, and A.-L. Barabási. Collective response of human populations to large-scale emergencies. *PLoS ONE*, 6(3):e17680, 03 2011.
- [7] S. Wasserman and K. Faust. *Social Network Analysis: Methods and Applications*. Cambridge University Press, 1994.
- [8] G. Di Battista, P. Eades, R. Tamassia, and I. G. Tollis. *Graph drawing: algorithms for the visualization of graphs*, volume 3. Prentice Hall New Jersey, USA, 1999.
- [9] M. Rosvall and C. T. Bergstrom. Maps of random walks on complex networks reveal community structure. *Proceedings of the National Academy of Sciences*, 105(4):1118, 2008.
- [10] S. Fortunato. Community detection in graphs. *Physics Reports*, 486(3-5):75–174, 2010.
- [11] J. Park, D.-S. Lee, and M. C. González. The eigenmode analysis of human motion. *Journal of Statistical Mechanics: Theory and Experiment*, 2010:P11021, 2010.
- [12] M. Kendall and J. D. Gibbons. *Rank Correlation Methods*. C. Griffin, 5th edition, 1990.